Available online at www.sciencedirect.com
ScienceDirect
Ceramics International 38S (2012) S529–S533
CERAMICS INTERNATIONAL
www.elsevier.com/locate/ceramint

Thermoelectric characteristics of the $(Bi,Sb)_2(Te,Se)_3$ nanocomposites processed with nanoparticle dispersion

M.Y. Kim, Y.H. Yeo, D.H. Park, T.S. Oh *

Department of Materials Science and Engineering, Hongik University, 72-1 Sangsu-dong, Mapo-gu, Seoul 121-791, Republic of Korea

Available online 24 May 2011

Abstract

The p-type $(Bi_{0.2}Sb_{0.8})_2Te_3$ and the n-type $Bi_2(Te_{0.9}Se_{0.1})_3$ thermoelectric nanocomposites were processed with dispersion of multi-walled carbon nanotubes and Al_2O_3 nanopowders. The lattice thermal conductivity κ_{ph} of the p-type $(Bi,Sb)_2Te_3$ was effectively reduced from 0.64 W/m K to 0.45–0.54 W/m K by dispersion of carbon nanotubes. The room-temperature figure-of-merit of the p-type $(Bi,Sb)_2Te_3$ was improved from 3.37×10^{-4}/K to 3.52×10^{-4}/K with dispersion of 0.05 vol.% carbon nanotubes. The figure-of-merit of the n-type $Bi_2(Te,Se)_3$ at 75 °C was substantially improved from 2.9×10^{-4}/K to 3.5×10^{-4}/K with dispersion of 0.5 vol.% Al_2O_3 nanopowders.

Keywords: A. Hot pressing; B. Nanocomposites; C. Thermal conductivity; C. Thermoelectric properties

1. Introduction

With serious concerns regarding the exhaustion of fossil fuel resources and environmental pollution, there has been renewed interest in thermoelectric power generation, which can recycle the waste heat as an energy saving technology [1,2]. The energy conversion efficiency of thermoelectric devices depends partly on the figure-of-merit (Z) or the dimensionless figure-of-merit (ZT) of thermoelectric materials which is related to material parameters such as Seebeck coefficient α, electrical conductivity σ, and thermal conductivity κ ($Z = \alpha^2\sigma/\kappa$). The dimensionless figure-of-merits (ZT) of bulk thermoelectric materials have been stagnant at about 1 for the last several decades, limiting the widespread thermoelectric applications [1–3].

In the last decade, much attention was focused on low-dimensional thermoelectric structures of which figure-of-merits were predicted to improve significantly compared with those of bulk thermoelectric materials due to quantum-confinement effects [1,4–6]. Significant enhancements in ZT values have been experimentally achieved in the superlattice devices of Bi_2Te_3/Sb_2Te_3, PbTe/PbSeTe, and Si/Ge [4–6]. However, such low-dimensional thermoelectric devices would have limited applications for large-scale energy-conversion, because they are too thin to support appreciable temperature differentials [1,2]. Because of the disadvantages of low-dimensional thermoelectric structures for large-scale applications, researches have been extensively focused on nanocomposites to realize nanoscale thermoelectric enhancement in bulk thermoelectric materials [1,3,7–9]. Dispersion of nanoparticles into thermoelectric materials has been suggested to improve the figure-of-merit by decreasing the lattice thermal conductivity without adversely affecting the electrical resistivity [8–10].

As p-type $(Bi,Sb)_2Te_3$ and n-type $Bi_2(Te,Se)_3$ possess superior thermoelectric characteristics around room temperature, they have been extensively utilized for low-temperature thermoelectric generation as well as Peltier cooling.

In this study, p-type $(Bi,Sb)_2Te_3$ and n-type $Bi_2(Te,Se)_3$ nanocomposites were processed by hot pressing with dispersion of nanopowders and their thermoelectric characteristics were evaluated.

2. Experimental

To fabricate p-type $(Bi,Sb)_2Te_3$ nanocomposites, appropriate amounts of Bi, Sb, and Te granules (>99.99%) were weighed for the $(Bi_{0.2}Sb_{0.8})_2Te_3$ composition and charged with multi-walled

* Corresponding author. Tel.: +82 2 320 1655; fax: +82 2 333 0127.
E-mail address: ohts@hongik.ac.kr (T.S. Oh).

0272-8842/$36.00
doi:10.1016/j.ceramint.2011.05.069

carbon nanotubes (CNTs) up to 0.25 vol.% in a hardened tool steel vial under Ar atmosphere. Steel balls were also charged as milling media and a ball-to-material weight ratio was held at 10:1. Mechanical alloying was conducted by shaking the vial at 1200 rpm for 5 h using a Spex mixer/mill (SPEX SamplePre-8000M, USA). After the vibro-milling process, X-ray diffraction analysis (RIGAKU ULTIMA IV, Japan) was performed to confirm the complete formation of the $(Bi,Sb)_2Te_3$ powders. The mechanically alloyed powers were cold pressed at 10 MPa to form 5 mm × 5 mm × 10 mm compacts and hot pressing was conducted in vacuum at 550 °C for 30 min.

To fabricate n-type $Bi_2(Te,Se)_3$ nanocomposites, high purity (>99.99%) Bi, Te, and Se granules, weighed for the $(Bi_{0.9}Sb_{0.1})_2Te_3$ composition, were charged into a quartz tube and vacuum-sealed. The $Bi_2(Te,Se)_3$ alloy was melted at 700 °C for 2 h using a rocking furnace to ensure the composition homogeneity. The ingot was crushed to form $Bi_2(Te,Se)_3$ powders of 38–90 μm size. $Bi_2(Te,Se)_3$ powders were charged with 0.5 vol.% Al_2O_3 powders (40 nm diameter) in a hardened tool steel vial under Ar atmosphere. Mechanical milling was conducted at a ball-to-material weight ratio of 10:1 for 3 h. The mechanically milled powers were cold pressed at 10 MPa to form 5 mm × 5 mm × 10 mm compacts and then hot pressed in vacuum at 550 °C for 30 min.

Seebeck coefficient (α) of the hot-pressed specimens was measured (SEEPEL TEO1000, Korea) by applying a temperature difference of 10 °C at both ends of a specimen. Electrical resistivity (ρ) and thermal conductivity (κ) were measured by 4-point probe (SEEPEL TEP1000, Korea) and laser flash (NETZSCH LFA-457, Germany) methods, respectively. Figure-of-merit was evaluated using the relation of $Z = \alpha^2/(\rho\kappa)$. Microstructures of the p-type $(Bi,Sb)_2Te_3$ and n-type $Bi_2(Te,Se)_3$ nanocomposites were observed using scanning electron microscopy (HITACHI S-4300, Japan).

3. Results and discussion

Fig. 1 shows SEM micrographs of the p-type $(Bi,Sb)_2Te_3$ nanocomposites with CNT dispersion and Fig. 2 illustrates the

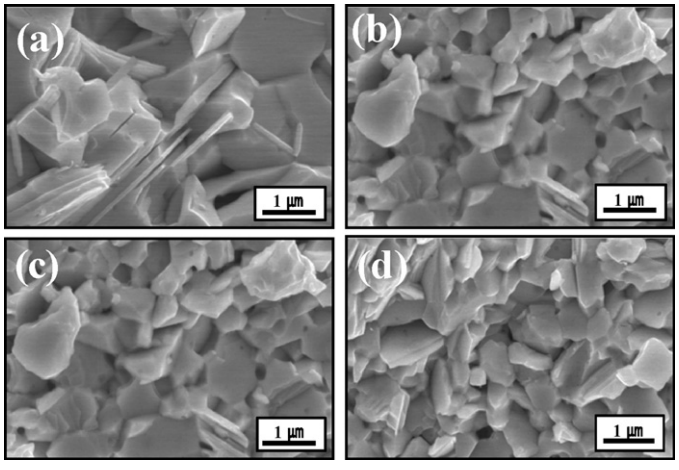

Fig. 1. SEM micrographs of the p-type $(Bi,Sb)_2Te_3$ dispersed with CNTs of (a) 0 vol%, (b) 0.05 vol%, (c) 0.15 vol%, and (d) 0.25 vol%.

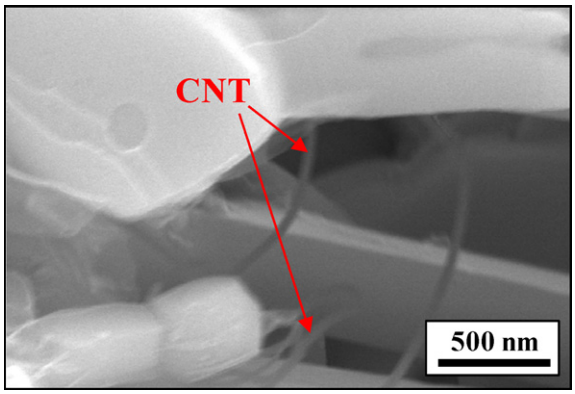

Fig. 2. SEM micrograph illustrating CNTs dispersed in the $(Bi,Sb)_2Te_3$ nanocomposite.

CNTs dispersed in the $(Bi,Sb)_2Te_3$ matrix. As shown in Fig. 1, the grain size of the hot-pressed $(Bi,Sb)_2Te_3$ decreased with CNT dispersion, which could be due to the inhibition of grain growth by dispersed CNTs. Maximum grain size D_{max} of the alloys with dispersion of second phase particles is limited to $4r/3f$, where r and f are the average radius and the volume fraction of second phase particles, respectively [11]. As shown in Fig. 1(b)–(d), differences in the grain size of the $(Bi,Sb)_2Te_3$ nanocomposites were not noticeable even with increasing the CNT content from 0.05 vol.% to 0.25 vol.%, implying that dispersion of CNTs was not uniform. Fig. 3 illustrates the relative density of the $(Bi,Sb)_2Te_3$ nanocomposites as a function of the CNT content. The relative density decreased slightly from 95.8% to 92.8% with dispersion of CNTs up to 0.25 vol.%.

Fig. 4 represents the Seebeck coefficient, electrical resistivity, thermal conductivity, and figure-of merit of the p-type $(Bi,Sb)_2Te_3$ nanocomposites, measured at 25 °C, as a function of the CNT content. The Seebeck coefficient and the electrical resistivity increased with dispersion of CNTs, which could be partly caused by reduction of the carrier mobility due to smaller grain size of the CNT-dispersed $(Bi,Sb)_2Te_3$

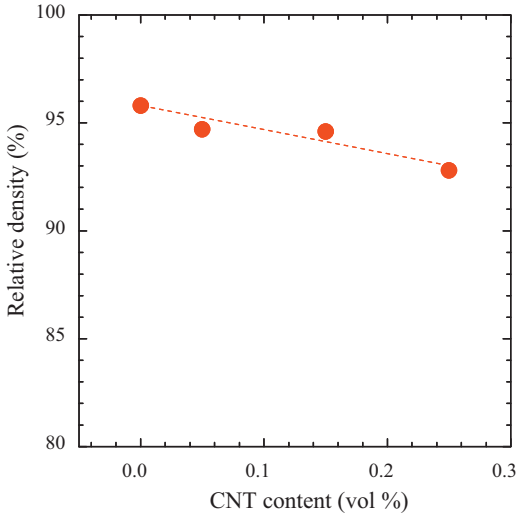

Fig. 3. Relative density of the p-type $(Bi,Sb)_2Te_3$ nanocomposites as a function of the CNT content.

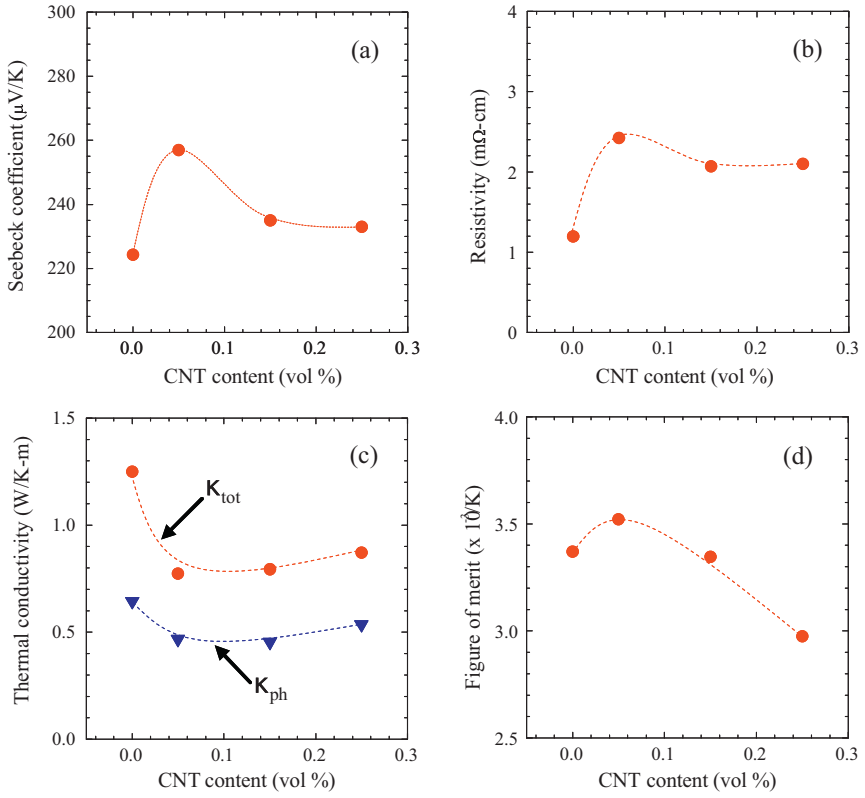

Fig. 4. (a) Seebeck coefficient, (b) electrical resistivity, (c) thermal conductivity, and (d) figure-of-merit, measured at 25 °C, of the p-type $(Bi,Sb)_2Te_3$ nanocomposites as a function of the CNT content.

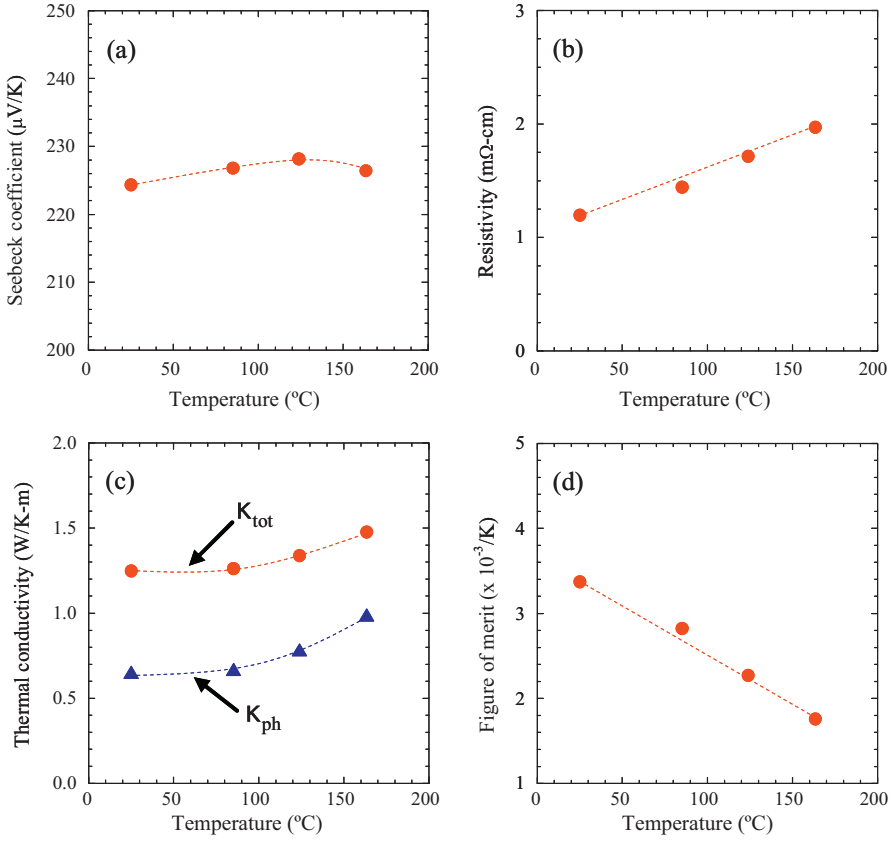

Fig. 5. Temperature dependences of (a) Seebeck coefficient, (b) electrical resistivity, (c) thermal conductivity, and (d) figure-of-merit of the p-type $(Bi,Sb)_2Te_3$ hot-pressed without CNT dispersion.

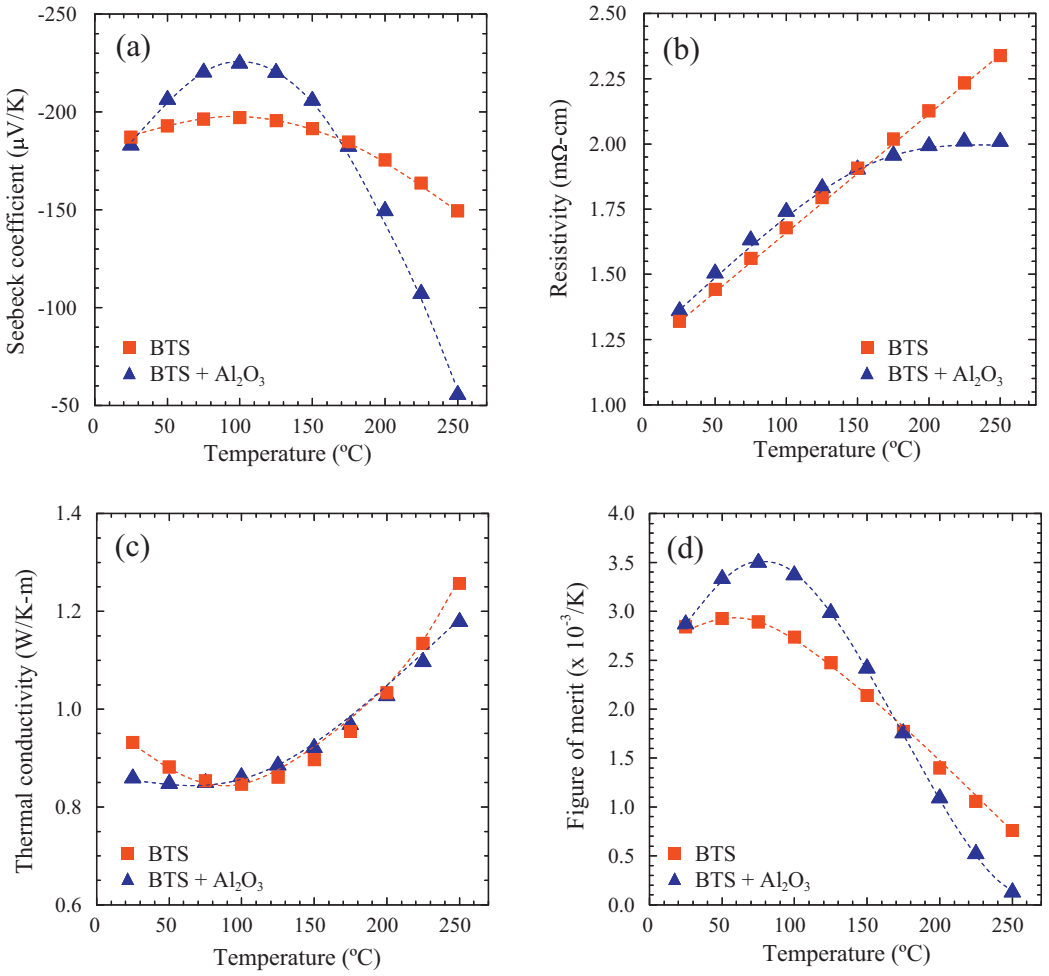

Fig. 6. Temperature dependences of (a) Seebeck coefficient, (b) electrical resistivity, (c) thermal conductivity, and (d) figure-of-merit of the $Bi_2(Te,Se)_3$ and the 0.5 vol.% Al_2O_3-dispersed $Bi_2(Te,Se)_3$.

nanocomposites. The Seebeck coefficient and the electrical resistivity decreased with increasing the CNT content from 0.05 vol.% to 0.25 vol.%, which could be attributed to the conducting nature of multi-walled carbon nanotubes. From the same variation behavior of the Seebeck coefficient as that of the electrical resistivity, it could be confirmed that the $(Bi,Sb)_2Te_3$ nanocomposites exhibited the extrinsic conduction at room temperature. As shown in Fig. 3(c), the total thermal conductivity decreased from 1.25 W/m K to 0.77–0.87 W/K m by CNT dispersion. For thermoelectric materials in extrinsic conduction region, the total thermal conductivity (κ_{tot}) can be expressed as $\kappa_{tot} = \kappa_{el} + \kappa_{ph}$ where κ_{el} is the electrical contribution to the thermal conductivity and κ_{ph} is the lattice thermal conductivity [12]. κ_{el} is also expressed as $\kappa_{el} = L\sigma T$ where L is the Lorenz number and σ is the electrical conductivity [12]. The lattice thermal conductivity κ_{ph} of the $(Bi,Sb)_2Te_3$ nanocomposites was obtained by calculating κ_{el} and subtracting κ_{el} from κ_{tot}. The lattice thermal conductivity κ_{ph} was effectively reduced from 0.64 W/K m to 0.45–0.54 W/K m by phonon scattering enhancement due to dispersion of CNTs. As shown in Fig. 3(d), the figure-of-merit of the p-type $(Bi,Sb)_2Te_3$ was improved from 3.37×10^{-4}/K to 3.52×10^{-4}/K with dispersion of 0.05 vol.% CNT.

Fig. 5 shows temperature dependences of the Seebeck coefficient, electrical resistivity, thermal conductivity, and figure-of merit of the $(Bi,Sb)_2Te_3$ hot-pressed without CNT dispersion. The electrical resistivity increased with increasing the measuring temperature up to 165 °C, indicating that the hot-pressed $(Bi,Sb)_2Te_3$ had the extrinsic conduction at this temperature range. The hot-pressed $(Bi,Sb)_2Te_3$ exhibited 1.25–1.45 W/K m and 0.64–0.97 W/K m as the total thermal conductivity and the lattice thermal conductivity, respectively. As reported for the CNT-dispersed n-type $Bi_2(Te,Se)_3$ nanocomposites [13], temperature dependences of the thermoelectric properties of the p-type $(Bi,Sb)_2Te_3$ would also be little changed with CNT dispersion. As shown in Fig. 5(d), the figure-of-merit exhibited a maximum at 25 °C and decreased with increasing the measuring temperature mainly due to the electrical resistivity increment, implying that the $(Bi_{0.2}Sb_{0.8})_2Te_3$ composition is more appropriate for Peltier cooling applications than for power generation applications.

Fig. 6 represents temperature dependences of the Seebeck coefficient, electrical resistivity, thermal conductivity, and figure-of merit of the n-type $Bi_2(Te_{0.9}Se_{0.1})_3$ nanocomposite dispersed with 0.5 vol.% Al_2O_3. The Seebeck coefficient was improved with the increase in the electrical resistivity by

dispersion of Al_2O_3. Compared to the p-type $(Bi,Sb)_2Te_3$ nanocomposites dispersed with CNTs, the resistivity increase could be kept minimal by dispersing 0.5 vol.% Al_2O_3. As shown in Fig. 6(d), the figure-of-merit at 75 °C was substantially improved from 2.9×10^{-4}/K to 3.5×10^{-4}/k with dispersion of 0.5 vol.% Al_2O_3. The relative density of the hot-pressed $Bi_2(Te_{0.9}Se_{0.1})_3$ was not affected by 0.5 vol.% Al_2O_3 dispersion. The $Bi_2(Te_{0.9}Se_{0.1})_3$ hot-pressed without and with 0.5 vol.% Al_2O_3 dispersion exhibited the relative densities of 95% and 94.7%, respectively. It has been expected that the figure-of-merits of SiGe- and Bi_2Te_3-based alloys can be improved for 10–40% and 15–20%, respectively, with fine dispersion of ceramic powders as phonon scattering centers [8–10]. With the results obtained for the p-type $(Bi,Sb)_2Te_3$ and the n-type $Bi_2(Te,Se)_3$ nanocomposites, it can be suggested that nanodispersion of proper amount is an effective way to improve the figure-of-merit of bulk thermoelectric materials.

4. Conclusion

The p-type $(Bi,Sb)_2Te_3$ nanocomposites dispersed with CNTs were formed by utilizing mechanical alloying and hot pressing. The Seebeck coefficient and the electrical resistivity of the $(Bi,Sb)_2Te_3$ increased with dispersion of CNTs partly due to smaller grain size of the CNT-dispersed $(Bi,Sb)_2Te_3$ nanocomposites. The lattice thermal conductivity κ_{ph} of the $(Bi,Sb)_2Te_3$ was effectively reduced from 0.64 W/m K to 0.45–0.54 W/m K by CNT dispersion. The figure-of-merit of the p-type $(Bi,Sb)_2Te_3$ was improved from 3.37×10^{-4}/K to 3.52×10^{-4}/K with dispersion of 1 vol.% CNT. The figure-of-merit of the n-type $Bi_2(Te,Se)_3$ at 75 °C was substantially improved from 2.9×10^{-4}/K to 3.5×10^{-4}/k with dispersion of 0.5 vol.% Al_2O_3. With the results obtained for the p-type $(Bi,Sb)_2Te_3$ and the n-type $Bi_2(Te,Se)_3$ nanocomposites, it can be suggested that nanodispersion of proper amount is an effective way to improve the figure-of-merit of bulk thermoelectric materials.

Acknowledgements

This work was supported by the Energy Efficiency & Resources Development Project of the Korea Institute of Energy Technology Evaluation and Planning (KETEP) grant funded by the Ministry of Knowledge Economy, Republic of Korea (Project No.: 2008EID11P050000).

References

[1] B. Poudel, Q. Hao, Y. Ma, Y. Lan, A. Minnich, B. Yu, X. Yan, D. Wang, A. Muto, D. Vashaee, X. Chen, J. Liu, M.S. Dresselhaus, G. Chen, Z. Ren, High-thermoelectric performance of nanostructured bismuth antimony telluride bulk alloys, Science 320 (2008) 634–638.

[2] T.S. Oh, Thermoelectric characteristics of p-Type $(Bi,Sb)_2Te_3$/(Pb,Sn)Te functional gradient materials with variation of the segment ratio, Journal of Electronic Materials 38 (2009) 1041–1047.

[3] M.S. Dresselhaus, G. Chen, M.Y. Tang, R. Yang, H. Lee, D. Wang, Z. Ren, J.-P. Fleurial, P. Gogna, New directions for low-dimensional thermoelectric materials, Advanced Materials 19 (2007) 1–12.

[4] R. Venkatasubramanian, E. Siivola, T. Colpitts, B. O'Quinn, Thin-film thermoelectric devices with high room-temperature figures of merit, Nature 413 (2001) 597–602.

[5] T.C. Harman, P.J. Taylor, M.P. Walsh, B.E. Laforge, Quantum dot superlattice thermoelectric materials and devices, Science 297 (2002) 2229–2232.

[6] T. Koga, S.B. Cronin, M.S. Dresselhaus, J.L. Liu, K.L. Wang, Experimental proof-of-principle investigation of enhanced Z DT in (0 0 1) oriented Si/Ge superlattice, Applied Physics Letters 77 (2000) 1490–1492.

[7] K.F. Hsu, S. Loo, F. Guo, W. Chen, J.S. Dyck, C. Uher, T. Hogan, E.K. Polychroniadis, M.G. Kanatzidis, Cubic AgPbmSbTe2+m: bulk thermoelectric materials with high figure of merit, Science 303 (2004) 818–821.

[8] X.B. Zhao, X.H. Ji, Y.H. Zhang, J.P. Tu, X.B. Zhang, Bismuth telluride nanotubes and the effects on the thermoelectric properties of nanotube containing nanocomposites, Applied Physics Letters 86 (2005) 062111–062113.

[9] H.L. Ni, X.B. Zhao, T.J. Zhu, X.H. Ji, J.P. Tu, Synthesis and thermoelectric properties of Bi_2Te_3 based nanocomposites, Journal of Alloys and Compounds 397 (2005) 317–321.

[10] G.A. Slack, M.A. Hussain, The maximum possible conversion efficiency of Si–Ge thermoelectric generators, Journal of Applied Physics 70 (1991) 2694–2718.

[11] D.A. Porter, K.E. Eastering, Phase Transformations in Metals and Alloys, Chapman & Hall, London, 1992.

[12] W.M. Yim, F.D. Rosi, Compound tellurides and their alloys for Peltier cooling—a review, Journal of Solid State Electronics 15 (1972) 1121–1138.

[13] D.H. Park, M.Y. Kim, T.S. Oh, Thermoelectric energy-conversion characteristics of the n-type Bi2(Te,Se)3 nanocomposites processed with carbon nanotube dispersion, Current Applied Physics, in press (2011).